Differentiation of histological subtypes in lung cancer with ^{18}F-FDG-PET 3-point imaging and kinetic analysis

Tatsuro Tsuchida[1] MD,
Yoshiki Demura[2] MD,
Masato Sasaki[3] MD,
Miwa Morikawa[4] MD,
Yukihiro Umeda[4] MD,
Tetsuya Tsujikawa[5] MD,
Takashi Kudoh[5] MD,
Hidehiko Okazawa[5] MD,
Hirohiko Kimura[1] MD

1. Department of Radiology, University of Fukui, Japan
2. Department of Respiratory Medicine, Ishikawa Prefectural Central Hospital Kanazawa, Ishikawa, Japan
3. Department of Thoracic Surgery
4. Department of Respiratory Medicine, Faculty of Medicine, and
5. Biomedical Imaging Research Center, University of Fukui, Japan

***

Keywords: ^{18}F-FDG-PET/CT
- 3-point imaging
- Lung cancer
- Kinetic analysis
- Histological subtypes

Correspondence address:
Tatsuro Tsuchida, M.D.
Department of Radiology,
Faculty of Medical Sciences,
University of Fukui, Japan

Received:
25 June 2011
Accepted:
15 July 2011

Abstract

The purpose of this study was to evaluate differences in histological subtypes of lung cancer using ^{18}F-FDG-PET 3-point imaging and kinetic analysis. *Subjects* comprised 44 patients with histologically proven lung cancer (squamous cell carcinoma (SCC), n=18; well-differentiated adenocarcinoma (WDA), n=9; poorly/moderately differentiated adenocarcinoma (non-WDA), n=17) who underwent ^{18}F-FDG-PET/CT examinations at 1, 2h and 3 h after injection of 185MBq of ^{18}F-FDG, approximately. Mean standardized uptake value (SUV) in each lesion was measured at each time point and the increase rate of SUV (IR_SUV) was calculated. SUV and IR_SUV were compared among the 3 groups. In addition, to estimate differences in kinetic parameters for each group, kinetic analysis based on a 3-compartment model was performed. *Our results* showed SUV differed significantly at every time point among the 3 groups. IR_SUV between 2 and 3 h post-injection (IR_SUV_{2-3}) differed significantly among the 3 groups, while both IR_SUV_{1-3} and IR_SUV_{1-2} were significantly higher in SCC than in WDA. In kinetic analyses, both K1 and k3 showed significant differences among the 3 groups, with highest values in SCC and lowest in WDA. *In conclusion*, ^{18}F-FDG-PET 3-point imaging and kinetic analysis enabled the differentiation of histological subtypes in lung cancer, arising from differences in glucose transporter density and enzymatic activity of hexokinase.

Hell J Nucl Med 2011; 14(3): 224-227 *Published on line: 10 November 2011*

Introduction

Positron emission tomography (PET) using 2-deoxy-2-fluorine-18-fluoro-D-glucose (^{18}F-FDG) is an established diagnostic tool for oncological imaging [1]. In particular, dual-point ^{18}F-FDG-PET is reportedly useful for differentiating between malignant and benign lesions in various organs [2-9]. As for the differentiation of histological subtypes in malignancy, Mavi et al. (2006) [8] reported that differentiation between invasive and noninvasive ductal carcinoma in breast cancer was feasible using dual-point ^{18}F-FDG-PET. Others reported a positive correlation between dual time point changes and degree of cellular differentiation in lung cancer [5], but failed to achieve histological differentiation between squamous cell carcinoma (SCC) and poorly/moderately differentiated adenocarcinoma (unpublished data). Uptake of ^{18}F-FDG in malignancy is known to increase over the course of numerous hours [10], but the increment gradually becomes smaller. This indicates that the scan interval between 1 and 3h after injection of ^{18}F-FDG as used by others may be inappropriate for such differentiation and a different scan interval may be more appropriate. Therefore, this study tried to achieve differentiation using emission scans between 1 and 3h after ^{18}F-FDG injection.

As for the difference in factors that affect ^{18}F-FDG uptake in different histological subtypes, some investigations using immunohistochemistry have been reported [11-15]. In this respect, we also tried to reveal differences in these factors using kinetic analysis based on a 3-compartment model, instead of immunohistochemistry.

Subjects and methods

Patients

Subjects comprised 44 patients with lung cancer (SCC, n=18; well-differentiated adenocarcinoma (WDA), n=9; moderately/poorly differentiated adenocarcinoma (non-WDA), n=17). Histological confirmation was achieved by surgery or transbroncheal lung biopsy. Patient characteristics are shown in Table 1 in detail. Written informed consent was obtained from all patients participating in this study, which was approved by the institutional review board of the University of Fukui Hospital.

Table 1. *Patient characteristics*

		SCC	non-WDA	WDA
Patients		18	17	9
	male : female	18 : 0	11 : 6	5 : 4
Age (years)	mean ±SD	69.3±8.5	65.8±11.8	72.0±5.0
	range	53 - 83	44 - 82	64 - 80
Maximum diameter (mm)		48.9±17.9*	26.8 ± 10.1	27.2±21.8
	range (mm)	23 - 88	17 - 56	10 - 81
Stage	Ia	2	3	8
	Ib	0	2	1
	IIa	1	0	0
	IIb	0	0	0
	IIIa	5	0	0
	IIIb	5	4	0
	IV	5	8	0

** P<0.05 vs. WDA, non-WDA*

^{18}F-FDG-PET/ CT examination

All patients underwent ^{18}F-FDG-PET/CT examination using a PET/CT scanner (Discovery LS; General Electric Medical Systems, Waukesha, WI). Thirty-five transaxial images were acquired simultaneously per field of view with an interslice spacing of 4.25mm. This PET/CT scanner incorporates an integrated 4-slice multidetector CT scanner, which was used for attenuation correction. CT scanning parameters were as follows: Auto mA (upper limit, 40mA; noise index, 20); 140kV; section thickness, 5mm; table feed, 15mm; and pitch, 4.

After fasting for ≥6h, patients received intravenous administration of 185MBq of ^{18}F-FDG, then image acquisition was started 1, 2, and 3h after injection. A whole-body emission scan was performed from the head to the inguinal region with 2min per bed position (7-8 bed positions) for 1- and 3h imaging. Emission scan only in the chest region (1 or 2 bed positions to cover the lung cancer) was performed for 2h imaging. A transmission scan with CT was performed prior to each emission scan.

Image reconstruction

For attenuation correction, CT images were created with a matrix size of 512×512 before conversion to 128×128 matrices to correspond to PET emission images, then applied to emission data. The attenuation-corrected emission images were reconstructed with an ordered-subset expectation maximization (OSEM) iterative reconstruction algorithm (2 iterations, 14 subsets). Reconstructed images were converted to standardized uptake value (SUV) images according to patient body weight and injected dose of ^{18}F-FDG.

Data analysis

Irregular regions of interests (ROI) were drawn on the CT image slice showing the maximum diameter of lung cancer, so that the line of ROI traced the contours of the lesion. ROI were then copied on ^{18}F-FDG-PET images of identical CT slices and mean SUV (average of all pixels within the ROI) was measured. Increase rate of SUV (IR_SUV) was measured according to the following formula:

$IR\_SUV_{1-2} = (SUV_2 - SUV_1) \times 100 / SUV_1$

where SUV_1 represents SUV obtained at 1h post injection. For example, IR_SUV_{1-3} means the IR_SUV between 1h and 3h post injection.

At each time point SUV and at each time interval IR_SUV were compared among the 3 groups.

Kinetic analysis based on the 3-compartment model of ^{18}F-FDG proposed by others [16] was performed in all cases. In this analysis simulated input function generated from a standardized input function curve with body weight correction was used as reported by others [17] as neither arterial blood sampling nor dynamic scans on the left ventricle were performed in this study. Simulated input function was extrapolated until 3h post injection, with exponential fitting. With the simulated input function and individual tissue activity in each time point, a fitting procedure was performed. To simplify fitting parameters, the ratio between influx and efflux of ^{18}F-FDG (K1/k2) was fixed to 0.55, in accordance with a previous report [18].

Statistical analysis

Results are expressed as mean±SD. Differences in individual SUV, IR_SUV, and kinetic parameters among the 3 groups were compared using one-way ANOVA. Values of $P<0.05$ were considered statistically significant.

Results

Comparisons of SUV and IR_SUV among the 3 groups are shown in Figures 1 and 2, and Table 2. Serial changes to SUV in each group are demonstrated in Figure 1. Significant differences in SUV at each time point among the 3 groups were observed (Table 2). As for comparisons of IR_SUV, values were higher in SCC than in WDA for every time interval and IR_SUV_{2-3} allowed discrimination between the 3 groups (Fig. 2). Table 3 shows the results of kinetic analysis. Both K1 and k3 differed significantly among the 3 groups, and were highest in SCC and lowest in WDA. Figure 3 shows the simulated time-activity curves for each group.

Discussion

In the present study, SUV at each time point and IR_SUV_{2-3} were able to differentiate between histological subtypes of lung cancer. Others have already reported differentiation of histological subtypes of breast cancer using dual-point imaging [8]. In that report, invasive and noninvasive ductal cancers were differentiated by dual-point ^{18}F-FDG-PET imaging. Among lung cancer patients, others reported that dual-point ^{18}F-FDG-PET examination showed a positive correlation between SUV increase and degree of cellular differentiation [5].

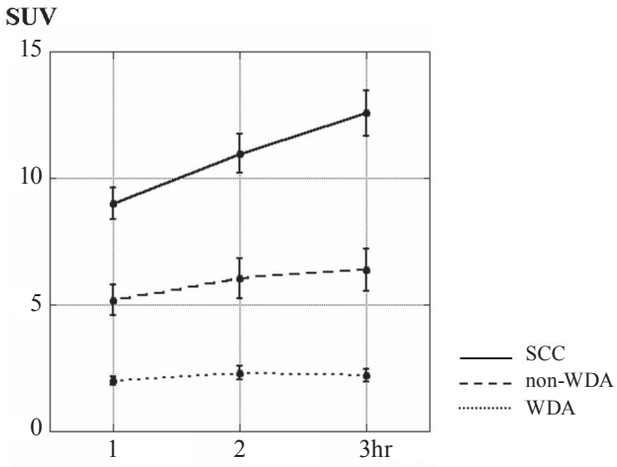

Figure 1. Gradual change in SUV for each group. SUV in SCC increased almost linearly during the scan period. However, SUV in WDA was almost constant.

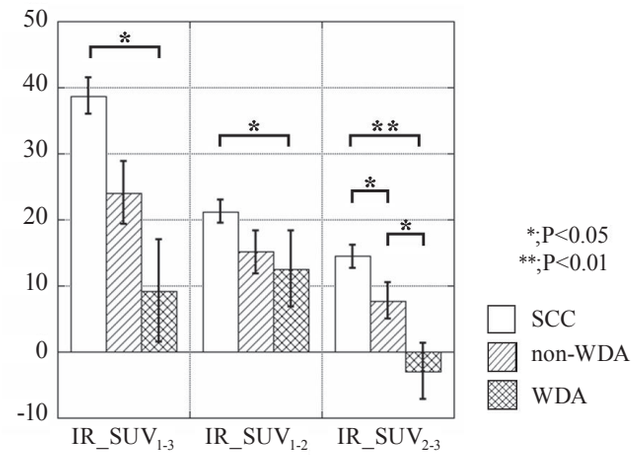

Figure 2. Comparison of IR_SUV in each scan interval. IR_SUV2-3 differed significantly among the 3 groups.

Table 2. *Comparison of SUV and IR_SUV among the 3 groups*

	SUV_1	SUV_2	SUV_3
SCC	9.0±2.6	11.0±3.3	12.6±3.7
non-WDA	5.2±2.5	6.1±3.3	6.4±3.4
WDA	2.0±0.5	2.3±0.8	2.2±0.7
	IR_SUV_{1-3}	IR_SUV_{1-2}	IR_SUV_{2-3}
SCC	38.7±11.8	21.2±7.4	14.5±7.4
non-WDA	24.0±19.6	15.1±13.5	7.8±11.2
WDA	9.2±23.2	12.6±17.4	-3.0±12.8

However, unpublished data from the same patient population showed no significant difference in IR_SUV_{1-3} between SCC and non-WDA (50.4±24.3% in 15 SCCs, 41.3±18.9% in 10 non-WDAs). In the present study, IR_SUV_{2-3} was able to differentiate between SCC and non-WDA, although neither IR_SUV_{1-3} nor IR_SUV_{1-2} could. Others reported that ^{18}F-FDG uptake in malignancy

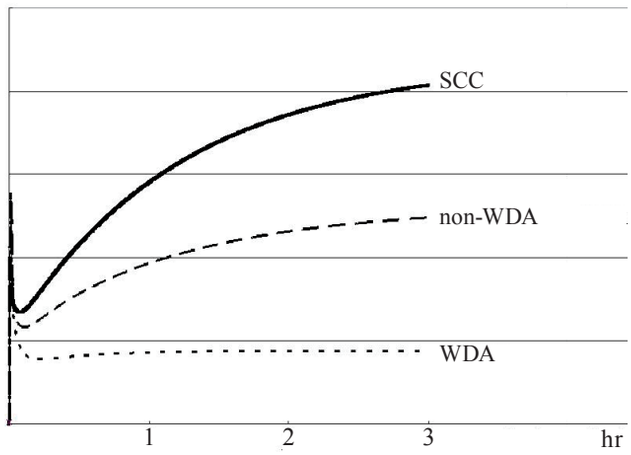

Figure 3. Simulated time-activity curves in each group. For this simulation, averaged K1 and k3 were used, as shown in Table 3.

Table 3. *Comparison of kinetic parameters among the 3 groups*

	K1	k3
SCC	0.105±0.029	0.116±0.034
non-WDA	0.06±0.028	0.067±0.034
WDA	0.022±0.006	0.023±0.007

increases for many hours, with a gradually decreasing increment [10]. In fact, IR_SUV_{2-3} was smaller than IR_SUV_{1-2} in all groups in our study, and the IR_SUV_{1-2} component in IR_SUV_{1-3} may negatively affect the statistical significance.

Several reports have examined the differentiation of histological subtypes in lung cancer with single-point ^{18}F-FDG-PET imaging [11-14, 19]. In those reports, ^{18}F-FDG uptake was higher in SCC than in adenocarcinoma. In particular, others reported that SUV differed significantly between SCC, bronchioloalveolar cell carcinoma (BAC) and non-BAC, compatible with the present results [19]. In addition, to investigate factors affecting ^{18}F-FDG uptake in lung cancer, correlations between ^{18}F-FDG uptake and parameters obtained from immunohistochemistry have also been reported [11-15]. In those reports, ^{18}F-FDG uptake in cancer cells correlated with amounts of glucose transporter-1 (Glut-1) and hexokinase-II (HK-II). In the present study, as no immunohistochemical examinations were performed, we tried to estimate the above parameters by kinetic analysis. Fluorine-18-FDG is usually transported into the cell via glucose transporter, metabolized to FDG-6-phosphate by hexokinase and trapped within the cell. Considering ^{18}F-FDG kinetics using a compartment model, the 3-compartment model proposed by Phelps et al. was applied [16]. In this model, K1 and k3 represent glucose transporter density and hexokinase activity, respectively. As Glut-1 and HK-II are thought to be the main subtypes of glucose transporter and hexokinase in regulating glucose influx [11] and metabolism [20], respectively, differences in K1 and k3 for different histological subtypes in lung cancer represent differences in the amounts of Glut-1 and HK-II. Both K1 and k3 showed significant differences between SCC,

non-WDA, and WDA in this study, supporting previous immunohistochemical findings. In all groups, K1/k3 was similar and the rate-limiting step was indeterminable, again agreeing with previous findings [21]. In this kinetic analysis, some limitations exist. First, as the simulated input function, not a measured input function was used in this analysis, both K1 and k3 were only estimated values. However, the difference in cerebral metabolic rate of glucose calculated with simulated input function and that with measured input function was less than 3% [12], so the estimated values of K1 and k3 may not show a large degree of error compared with measured values. Second, to simplify fitting parameters, the ratio between influx and efflux of ^{18}F-FDG (K1/k2) was fixed because the number of tissue activity points was small. Previous studies have reported K1/k2 as 4 [10], 0.55 [18], 0.47 [21] and 0.2 [22], showing a high degree of variability. We selected a value of 0.55 for this study, as this value was reproducible and seemed reliable.

To the best of our knowledge, this is the first report concerning the successful differentiation of histological subtypes in lung cancer with multi-point ^{18}F-FDG-PET imaging and kinetic analysis. As for the clinical relevance of differentiating the histological subtypes, it seems not to have clinical relevance in pretreatment differentiation as the diagnosis will be made by histology regardless of the differentiation with imaging. However, when the chemo-/radio-therapy was applied in advanced stage lung cancer patients, the change of ^{18}F-FDG uptake or kinetic parameter may vary between histological subtype and the response evaluation criteria in each histological subtypes may be required. From such viewpoint, histological differentiation with multi-point imaging is thought to have the clinical relevance although the further study will be required. Moreover, to confirm the validity of the kinetic parameters, direct comparison of the parameters and results of immunohistochemistry for amounts of Glut-1 and HK-II is required.

In conclusion, the present study was able to differentiate between histological subtypes of lung cancer using ^{18}F-FDG-PET 3-point imaging and kinetic analysis. Differences in kinetic parameters between all groups were concordant with previously described results of immunohistochemistry.

The authors declare that they have no conflicts of interest.

Bibliography

1. Delbeke D. Oncological applications of FDG PET imaging. J *Nucl Med* 1999; 40: 1706-15.
2. Hustinx R, Smith RJ, Benard F et al. Dual point fluorine-18 fluorodeoxyglucose positron emission tomography: a potential method to differentiate malignancy from inflammation and normal tissue in the head and neck. *Eur J Nucl Med* 1999; 26: 1345-8.
3. Zhuang H, Pourdehnad M, Lambright ES et al. Dual point ^{18}F-FDG PET imaging for differentiating malignant from inflammatory prodesses. *J Nucl Med* 2001; 42: 1412-7.
4. Matthies A, Hickeson M, Cuchiara A et al. Dual point ^{18}F-FDG PET for the evaluation of pulmonary nodules. *J Nucl Med* 2002; 43: 871-5.
5. Demura Y, Tsuchida T, Ishizaki T et al. ^{18}F-FDG accumulation with PET for differentiation between benign and malignant lesions in the thorax. *J Nucl Med* 2003; 44: 540-8.
6. Kumar R, Loving VA, Chauhan A et al. Potential of dual-point imaging to improve breast cancer diagnosis with ^{18}F-FDG PET. *J Nucl Med* 2005; 46: 1819-24.
7. Nishiyama Y, Yamamoto Y, Fukunaga K et al. Dual-time-point ^{18}F-FDG PET for the evaluation of gallbladder caricinoma. *J Nucl Med* 2006; 47: 633-8.
8. Mavi A, Urhan M, Yu JQ et al. Dual point ^{18}F-FDG PET imaging detects breast cancer with high sensitivity and correlates well with histologic subtypes. *J Nucl Med* 2006; 47: 1440-6.
9. Tian R, Su M, Tian Y et al. Dual-time point PET/CT with ^{18}F-FDG for the differentiation of malignant and benign bone lesions. *Skeketal Radiol* 2009; 38: 451-8.
10. Hamberg LM, Hunter GJ, Alpert NM et al. The dose uptake ratio as an index of glucose metabolism: useful parameter or oversimplification? *J Nucl Med* 1994; 35: 1308-12.
11. Brown RS, Leung JY, Kison PV et al. Glucose transporters and FDG uptake in untreated primary human non-small cell lung cancer. *J Nucl Med* 1999; 40: 556-65.
12. Higashi K, Ueda Y, Sakurai A et al. Correlation of Glut-1 glucose transporter expression with ^{18}F-FDG uptake in non-small cell lung cancer. *Eur J Nucl Med* 2000; 27: 1778-85.
13. Mamede M, Higashi T, Kitaichi M et al. ^{18}F-FDG uptake and PCNA, Glut-1, and hexokinase-II expressions in cancers and inflammatory lesions of the lung. *Neoplasia* 2005; 7: 369-79.
14. de Gues-Oei LF, van Krieken JH, Aliredjo RP et al. Biological correlates of FDG uptake in non-small cell lung cancer. *Lung Cancer* 2007; 55: 79-87.
15. Marom EM, Aloia TA, Moore MB et al. Correlation of FDG-PET imaging with Glut-1 and Glut-3 expression in early-stage non-small cell lung cancer. *Lung Cancer* 2001; 33: 99-107.
16. Phelps ME, Huang SC, Hoffman EJ et al. Tomographic measurement of local cerebral glucose metabolic rate in humans with [F-18]2-fluoro-2-deoxy-D-glucose: validation of method. *Ann Neurol* 1979; 6: 371-88.
17. Tsuchida T, Sadato N, Yonekura Y et al. Noninvasive measurement of cerebral metabolic rate of glucose using standardized input function. *J Nucl Med* 1999; 40: 1441-5.
18. Minn H, Zasadny KR, Quint LE et al. Lung cancer: reproducibility of quantitative measurement for evaluating 2-[F-18]-fluoro-2-deoxy-D-glucose uptake at PET. *Radiology* 1995; 196: 167-73.
19. Aquino SL, Halpern EF, Kuester LB et al. FDG-PET and CT features fo non-small cell lung cancer based on tumor type. *Int J Mol Med* 2007; 19: 495-9.
20. Mathupala SP, Rempel A, Pedersen PL. Aberrant glycolytic metabolism of cancer cells: a remarkable coordination of genitec, transcriptional, post-transcriptional, and mulational events that lead to a critical role for type II hexokinase. *J Bioenerg Biomembr* 1997; 29: 339-43.
21. Torizuka T, Zasadny KR, Recker B et al. Untreated primary lung and breast cancers:correlation between ^{18}F-FDG kinetic rate constants and findings of in vitro studies. *Radiology* 1998; 207: 767-74.
22. Torizuka T, Nobezawa S, Momiki S et al. Short dynamic FDG-PET imaging protocol for patients with lung cancer. *Eur J Nucl Med* 2000; 27: 1538-42.